Journal of Tropical Pharmacy and Chemistry

Journal homepage: https://jtpc.farmasi.unmul.ac.id

In-Silico Screening of Mitragynine Derivates from the Genus Mitragyna Korth Targeting the Main Protease of the SARS-COV-2

Islamudin Ahmad[1,2]*, Nur Masyithah Zamruddin[1], M. Arifuddin[2], Yuspian Nur[2], Firzan Nainu[3]

[1]Department of Pharmaceutical Sciences, Faculty of Pharmacy, Universitas Mulawarman, Samarinda, East Kalimantan 75119, Indonesia
[2]Laboratory of Pharmaceutical Research and Development of FARMAKA TROPIS, Faculty of Pharmacy, Universitas Mulawarman, Samarinda, East Kalimantan 75119, Indonesia
[3]Faculty of Pharmacy, Hasanuddin University, Makassar, South Sulawesi 90245, Indonesia
*Corresponding author: islamudinahmad@farmasi.unmul.ac.id

Abstract

Coronavirus Diseases 2019, caused by SARS-CoV-2, has been a significant threat to global public health. Unfortunately, effective COVID-19 vaccines and clinically-proven anti-SARS-CoV-2 drugs remain unavailable. This study was carried out aiming to predict the potential effect of mitragynine derivates from the Genus Mitragyna Korth as an inhibitor of M^{pro}, the main protease of the SARS-CoV-2, by *in silico* molecular docking study. The crystal structure of the main protease of SARS-CoV-2 as an active site target was obtained from the PDB database (rcsb.org) with PDB ID: 5R84 and 6LU7 with the native ligand of Z31792168 and N3, respectively. The analysis of *in silico* molecular docking was conducted using Autodock 4.2.6 (100 docking runs). The central grid was placed on HIS41 and CYS145 with a grid box comprised of 40Å × 30Å × 34Å (for protein 5R84) and 36Å × 62Å × 40Å (for protein 6LU7) points spaced by 0.375 Å was centered on the active site of X=9.812Å; Y=-0.257Å; Z=20.849Å and X=-9.732Å; Y=11.403Å; X=68.483Å (XYZ-coordinates), respectively. Our research indicated that mitrjavine and ajmalicine exhibit greater potential inhibition of the active site on the M^{pro} of SARS-CoV-2, even stronger than native ligands. We believed that these compounds are promising candidates to be examined in further COVID-19 drug discovery studies.

Keywords: Ajmalicine, COVID-19, mitrajavine, mitragynine derivates, molecular docking, SARS-CoV-2

Received: 20 December 2022 **Accepted**: 10 May 2023

DOI: https://doi.org/10.25026/jtpc.v7i2.523

How to Cite:

Ahmad, I., Zamruddin, N. M., Arifuddin, M., Nur, Y., Nainu, F., 2023. *In-Silico* Screening of Mitragynine Derivates from the Genus Mitragyna Korth Targeting the Main Protease of the SARS-COV-2. *J. Trop. Pharm. Chem.* **7**(2). 78-89. **DOI**: https://doi.org/10.25026/jtpc.v7i2.523

1 Introduction

The Coronavirus Disease 2019 (COVID-19) pandemic had been listed as one of the major issues in global public health with 5,406,282 confirmed COVID-19 cases and 343,562 deaths [1]. Severe Acute Respiratory Syndrome Coronavirus 2 (SARS-CoV-2), a newly emerging coronavirus, has been reported as the cause of COVID-19. As a member of the *Coronaviridae* family, SARS-CoV-2 is equipped with a single-strand, positive-sense RNA genome, enveloped in a roughly spherical structure with a number of spike surface projections [2]. The virus is included in the beta-coronavirus (beta-CoV), one of the four genera of coronavirus [3,4]. In addition, SARS-CoV-2 is the seventh virus of the *Coronaviridae* family that has been known to infect humans after SARS-CoV, MERS-CoV, HKU1, OC43, NL63, and 229E [5]. Despite global efforts to discover safe and effective immunological and pharmacological interventions for COVID-19, clinically approved COVID-19 vaccines and antiviral drugs remain unavailable.

SARS-CoV-2 contains four structural proteins, include nucleocapsid protein (N), matrix glycoprotein (M), a small envelope protein (E), and spike glycoprotein (S) [6]. Spike glycoprotein of SARS-CoV-2 contains Receptor Binding Domain (RBD) that exhibits a critical function in the viral entry process to the targeted host cells [7]. The S protein is the main protease that plays an essential role in the viral replication cycle [8]. the main protease (M^{pro}) structure consists of three domains, domain I (residue 8-101), domain II (residue 102-184), and domain III (residue 201-306). Histidine 41 (in domain I) and Cysteine 145 (in domain II) are active protease sites. The main protease known as chymotrypsin-like cysteine protease (3CLpro) plays an essential role in mediating viral replication and transcription, making it an attractive drug target for COVID-19 treatment [9,10,11]. Indeed, inhibition of SARS-CoV-2 M^{pro} by certain protease inhibitors have been shown as a promising approach to disrupt viral propagation [12,13, 4]. The crystal 3D structure of the main protease domain-inhibitor complex is publicly available at Protein Data Bank (www.rcsb.org/), thus easily accessible for drug discovery *in silico* models [10,11,15]. Some clinically-proven drugs such as chloroquine, lopinavir, ritonavir, indinavir, saquinavir, and carfilzomib have been tested *in silico* on the main protease receptors of SARS-CoV-2 [11,15,16,17,18]. In addition, several natural product compounds such as hesperetin, glycyrrhirhizin, nicotianamine, scutellarin, and baicalein [19]; hispidin dan lepidine [20]; citrus and galangal constituents [21]; and a fungal metabolite-flaviolin [22], were also been screened for their pharmacological potential as SARS-CoV-2 protease inhibitors. On the other hand, indole alkaloid groups are one of the natural products that are widely studied as antiviral agents. Zhang et al. have reported the related developments and the current status of outstanding indole alkaloid groups in the field of antiviral drug discovery [23].

One of the critical indole alkaloids to be investigated for its potential to inhibit the action of the main protease of the SARS-CoV-2 is the mitragynine derivative of the genus Mitragyna Korth. The genus Mitragyna Korth has the main content of mitragynine derivatives [24]. Some studies have reported the pharmacological effects of these compounds [25,26,27,28]. However, a study related to activity as the M^{pro}

of the SARS-CoV-2 inhibitor has not been reported. This study aims to predict the potential of inhibitory activity of derivatives mitragynine on the M^{pro} of SARS-CoV-2 according to the free energy bonding and interaction conformation obtained from the in silico molecular docking results analysis.

2 Materials and Methods

2.1 Materials

In this study, *in silico* molecular docking study was performed using a computer with specification processor Intel® Core™ i5-5200U CPU @2.20 GHz 2.19 GHz, 4.00 GB memory DDR3 (ASUS®, Taiwan), NVIDIA GEFORCE 820 M VGA, Windows Education 10.1, 64-bit Operating system, Autodock v4.2.6 and AutodockTools (http://autodock.scrips.edu/), Phyton Molecular Viewer (PMV 1.5.6), Discovery Studio Visualizer, OpenBabel GUI, and ChemOffice Pro v15.00 PerkinElmer.

2.2 Preparation of native ligand and protein receptor

The protein structure of SARS-CoV-2 M^{pro} in complex with Z31792168 (PDB ID: 5R84, with 1.93Å resolution) and N3 (PDB ID: 6LU7, 2.16Å resolution) were downloaded from Protein Data Bank (rcsb.org/pdb/). Each native ligand and macromolecule protein receptor were separated using Phyton Molecular Viewer (PMV 1.5.6). Water molecules were eliminated from each protein receptor and protonated. Gasteiger charges were added to each ligand atom. Then a native ligand and protein receptor was prepared and converted in the PDBQT format (.pdbqt) using AutodockTools and OpenBabel programs [29,30].

2.3 Preparation of ligand sample

The structure of compounds from genus Mitragyna Korth was provided and documented by Brown and his colleague [24] (as illustrated in Figures 1). To preparing a ligand sample, ChemDraw® Pro 15 was used to build a 2D structure of each compound. Chem3D® Pro 15 was used to convert to 3D structure and minimized using the MMFF94 force field and save to PDB (.pdb) format [10].

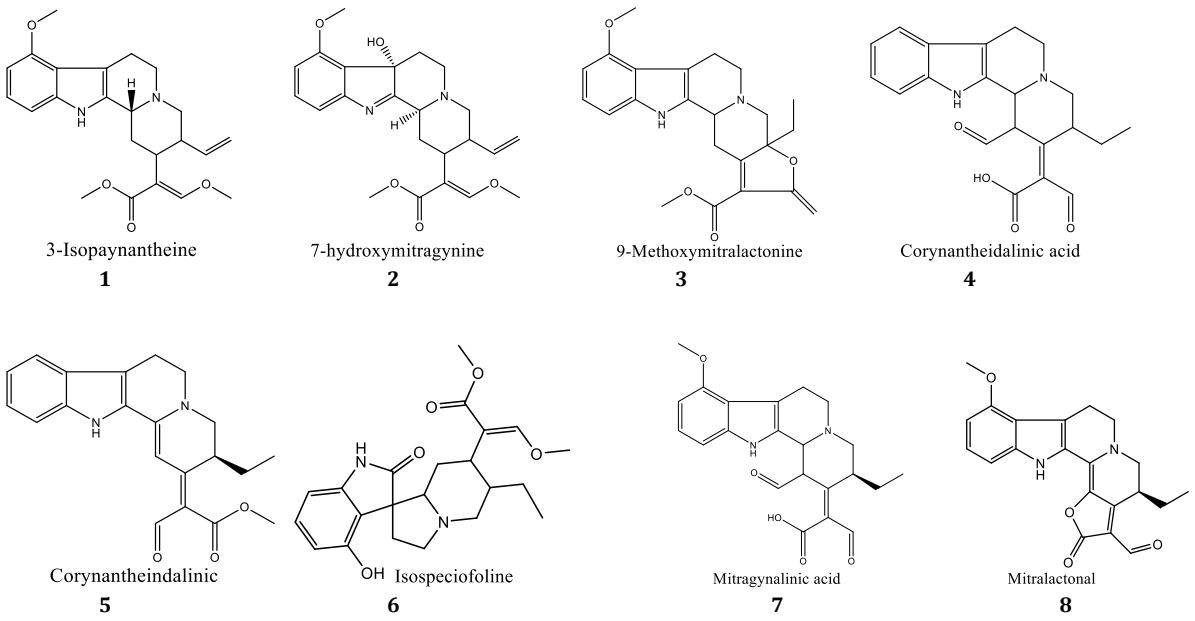

Figure 1. Mitragynine derivates (1-52)

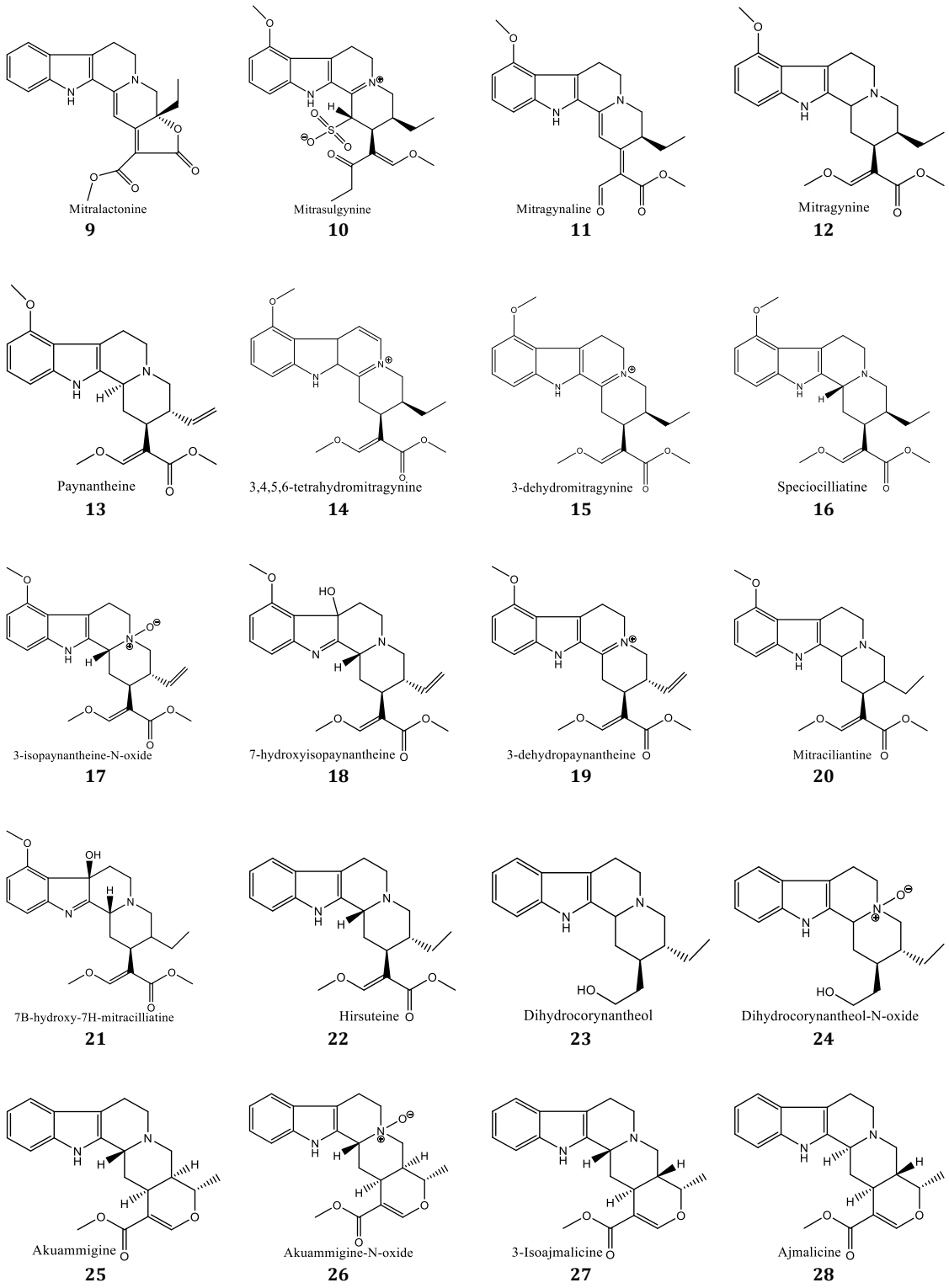

Figure 1. Mitragynine derivates (1-52)

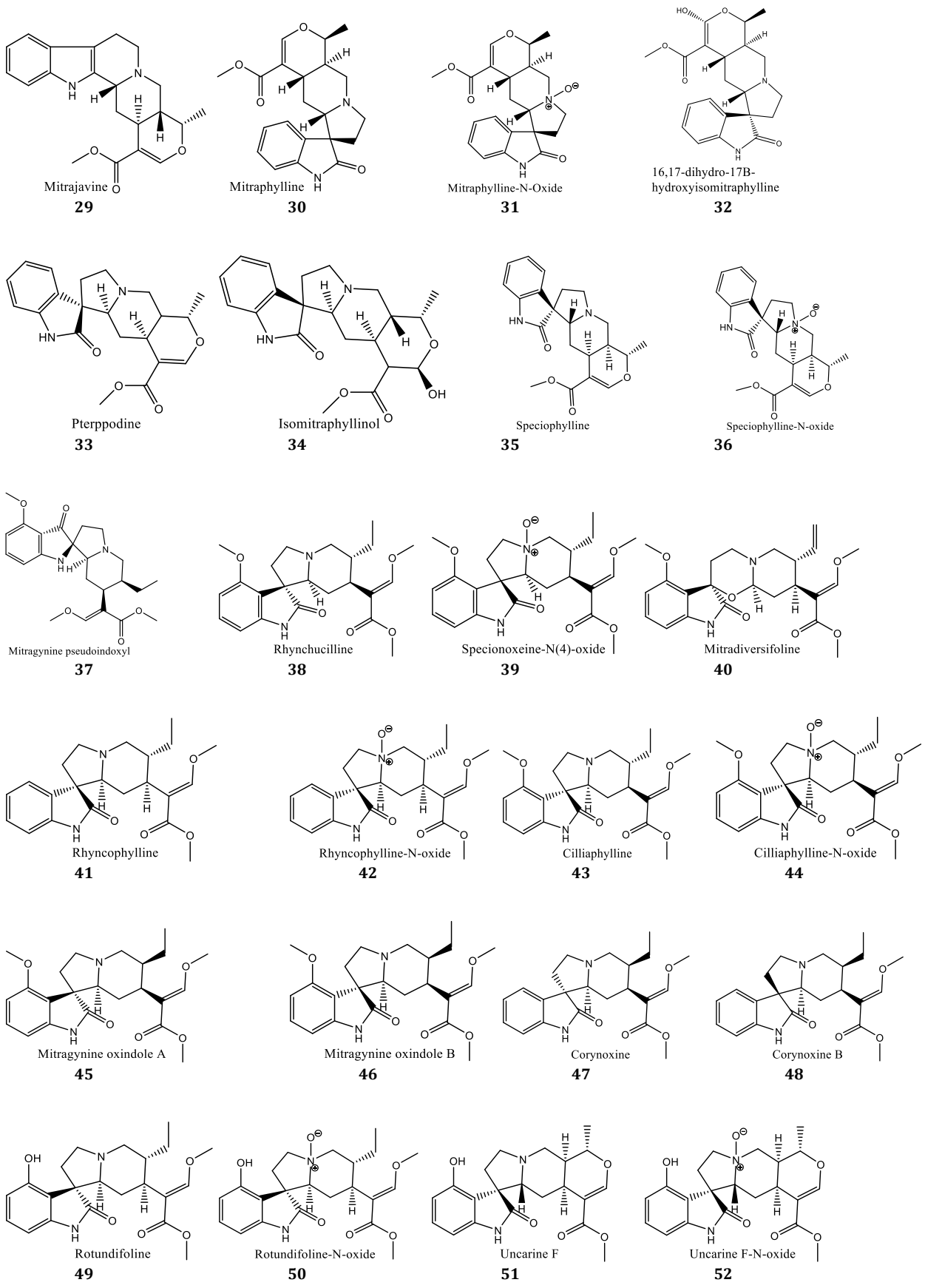

Figure 1. Mitragynine derivates (1-52)

2.4 Analysis of in silico molecular docking

Molecular docking analysis of 52 mitragynine derivatives was performed using Autodock 4.2.6 according to its protocols [30]. Each native ligand was simulated with some different conformation to obtain the best docking on binding site of protein receptor using a Lamarckian Genetic Algorithm (LGA) based on the lowest free energy of binding (ΔG). The parameters of LGA were: mutation rate of 0.02, crossover rate of 0.8, elitism of 1, the population size of 150, energy evaluation of 2500000, and 100 runs. Moreover, the grid box comprised of 40×30×34 (for protein 5R84) and 36×62×40 (for protein 6LU7) points spaced by 0.375Å was centered on the active site of X= 9.812Å; Y= -0.257Å; Z= 20.849Å and X= -9.732Å; Y= 11.403Å; X= 68.483Å (XYZ-coordinates), respectively. These grid conditions were used to docking analysis of 52 mitragynine derivative compounds. The results of docking data were visualized using Accelrys Discovery Studio Visualizer 4.0 [31].

3 Results and Discussion

In the present study, *in silico* molecular docking analysis of 52 compounds [24] was performed on the M^{pro} receptor of SARS-Cov-2. This work aims to predict the potential activity of mitragynine derivatives based on interaction and bond types with the receptor active site. The structure of the taget macromolecule of SARS-CoV-2 protease were obtained from Protein Data Bank at the website: https://rcsb.org (with PDB ID: 5R84 and 6LU7). Of these proteins, there are consists of 3 domains: domain I at residue 8-101, domain II at residue 102-184, and domain III at residue 185-200. The Histidine 41 (domain I) and Cysteine 145 (domain II) are the protease active site of SARS-CoV-2 [9]. Two proteins used as target receptors in this study, 5R84 and 6LU7, were actually the same main protease of SARS-CoV-2 with no different characteristics other than their corresponding native ligand; Z31792168 for 5R84 and N3 for 6LU7. The difference lies in the types and structure of both native ligands, as well as the conformation of bonds and interactions of protein residues, especially in the domain of the active site [9,32,15].

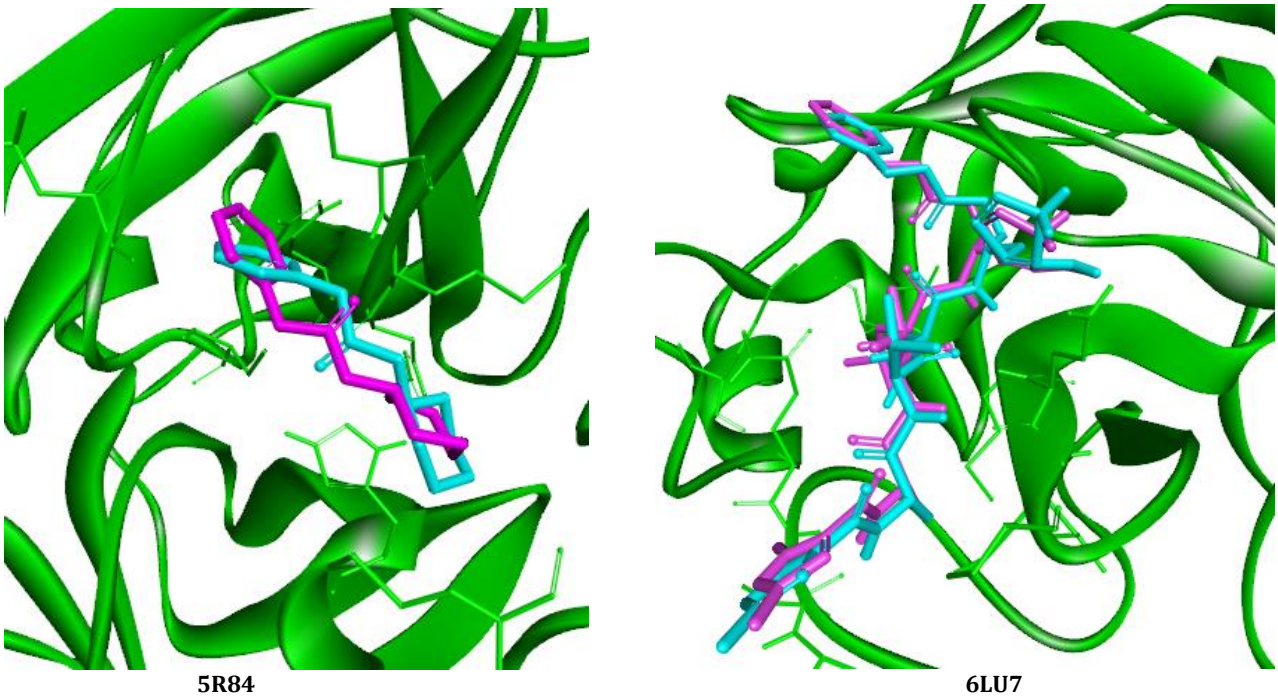

5R84 **6LU7**

Figure 2. Native ligand (purple) and native ligand re-docked (blue) comparisons.

Table 1. The molecular docking results of native ligand and Mitragynine Derivates

Ligand	Inhibition Constant (nM)		Free energy binding (kcal/mol)		Ligand	Inhibition Constant (nM)		Free energy binding (kcal/mol)	
	5R84	6LU7	5R84	6LU7		5R84	6LU7	5R84	6LU7
Native ligand-5R84 (Z31792168)	8640	-	-6.91	-	Akuammigine-N-oxide (26)	426.21	202.04	-8.69	-9.13
Native Ligand-6LU7 (N3)	-	186.57	-	-9.18	3-Isoajmalicine (27)	258.33	280.31	-8.99	-8.94
3-Isopaynantheine (1)	1090	3960	-8.13	-7.37	**Ajmalicine (28)**	**283.95**	**36.08**	**-8.93**	**-10.15**
7-Hydroxymitragynine (2)	17970	2930	-6.47	-7.55	**Mitrajavine (29)**	**249.11**	**31.89**	**-9.01**	**-10.23**
9-Methoxymitralactonine (3)	1580	1260	-7.91	-8.05	Mitraphylline (30)	5550	2710	-7.17	-7.60
Corynantheidalinic acid (4)	8560	1710	-6.91	-7.87	Mitraphylline-n-oxide (31)	2320	1630	-7.69	-7.90
Corynantheidalinic (5)	830	1650	-8.29	-7.89	16,17-dihydro-17β-hydroxyisomitraphylline (32)	2870	912.61	-7.87	-8.24
Isospeciofoline (6)	2720	10810	-7.59	-6.81	Pteropodine (33)	2820	950.11	-7.57	-8.22
Mitragynalinic acid (7)	11210	5490	-6.75	-7.18	Isomitraphyllinol (34)	24750	970.63	-6.28	-8.20
Mitralcatonal (8)	2370	1240	-7.67	-8.06	Speciophylline (35)	400.99	501.94	-8.73	-8.59
Mitralactonine (9)	1030	622.36	-8.17	-8.47	Speciophylline-N-oxide (36)	5610	2790	-7.16	-7.58
Mitrasulgynine (10)	11420	33000	-6.74	-6.11	Mitragynine pseudoindoxyl (37)	386.13	20.17	-4.66	-6.41
Mitragynaline (11)	12160	1240	-6.71	-8.06	Rhynchociline (38)	1700	2900	-7.87	-7.55
Mitragynine (12)	4120	1790	-7.35	-7.84	Specionoxeine-N(4)-oxide (39)	7140	13.03	-7.02	-6.66
Paynantheine (13)	1490	1840	-7.95	-7.82	Mitradiversifoline (40)	57430	9140	-5.79	-6.87
3,4,5,6-tetrahydromitragynine (14)	2460	3880	-7.65	-7.38	Rhyncophylline (41)	3720	6740	-7.41	-7.05
3-dehydromitragynine (15)	5440	1720	-7.18	-7.86	Rhyncophylline-N-oxide (42)	5680	4810	-7.16	-7.25
Speciociliatine (16)	25150	2820	-6.27	-7.57	Ciliaphylline (43)	2110	6340	-7.74	-7.09
3-Isopaynantheine (17)	3530	2880	-7.44	-7.60	Ciliaphylline-N-oxide (44)	11940	9220	-6.72	-6.87
7-Hydroxyisopaynantheine (18)	7440	2650	-7.00	-7.61	Mitragynine oxindole A (45)	45580	7530	-5.92	-6.16
3-dehydropaynantheine (19)	4310	1020	-7.32	-8.18	Mitragynine oxindole B (46)	15820	12730	-6.55	-6.68
Mitraciliatine (20)	3470	1860	-7.47	-7.82	Corynoxine (47)	2720	1310	-7.59	-8,02
7β-hydroxy-7H-mitraciliatine (21)	3.52	2630	-7.44	-7.61	Corynoxine B (48)	3740	7640	-7.40	-6.98
Hirusteine (22)	1300	776.50	-8.03	-8.34	Rotundifoline (49)	34270	18580	-6.09	-6.45
Dihydrocorynantheol (23)	2260	1260	-7.70	-8.05	Rotundifoline-N-oxide (50)	8200	8680	-6.94	-6.90
Dihydrocorynantheol-N-oxide (24)	1660	1310	-7.88	-8.03	Uncarine F (51)	4290	898.21	-7.32	-8.25
Akuammigine (25)	1390	421.73	-7.99	-8.70	Uncarine F-N-oxide (52)	6370	3900	-7.09	-7.38

On the SARS-CoV-2 protein receptor, both native ligands (Z31792168 from 5R84 and N3 from 6LU7) are converged to verify the RMSD value of the smallest energy of the backbone atoms and their interaction with the active site of the receptor. The docking results of Z31792168 (5R84) and N3 (6LU7) native ligand were obtained the value of root mean square deviation (RMSD) from reference structure of 1.112 and 0.978 Å (with RMSD tolerance of 2 Å) and clusters of 86 and 36 for 100 times running with a binding energy value of -6.91 and -9.18 kcal/mol (Figure 2).

The prediction of 52 compounds based on binding energy value and Inhibition constant calculation is shown in Table 1. As can be seen in Table 1, 40 of the total 52 compounds (in 5R84) displayed lower binding energy value than the native ligand Z31792168 (with a binding energy value of -6.81 kcal/mol and the inhibition constant 8640 nM or 8.64 μM). Whereas, in the assessment using protein of 6LU7 as target only two compounds (ajmalicine and mitrajavine) possessed the lowest binding energy value than the native ligand N3 (with -9.18 kcal/mol of binding energy and 186.57 nM of inhibition constant). Indeed, a similar observation was seen after careful checking of data obtained using the protein receptor of 5R84, mitrajavine, isoajmalicine, and ajmalicine had the lowest binding energy value of -9.01, -8.99, and -8.93 kcal/mol and the inhibition constant of 249.11, 258.33, and 283.95 nM, respectively. These three compounds had lower binding energy values than native ligands. Futhermore, using protein receptors of 6LU7 as target, mitrajavine, ajmalicine, and akuammigine-N-oxide demonstrated the lowest binding energy of -10.23, -10.15, and -9.13 with inhibition constant (31.89, 36.09, and 202.04 nM), respectively. Based on these results, mitrajavine and ajmalicine compound demonstrated aprospective inhibitory activities to SARS-CoV-2 main protease (5R84 and 6LU7). It is important to note that these two compounds have structure but only differ in the hydrogen atom position (as can be seen in Figures 1, compound 28 and 29).

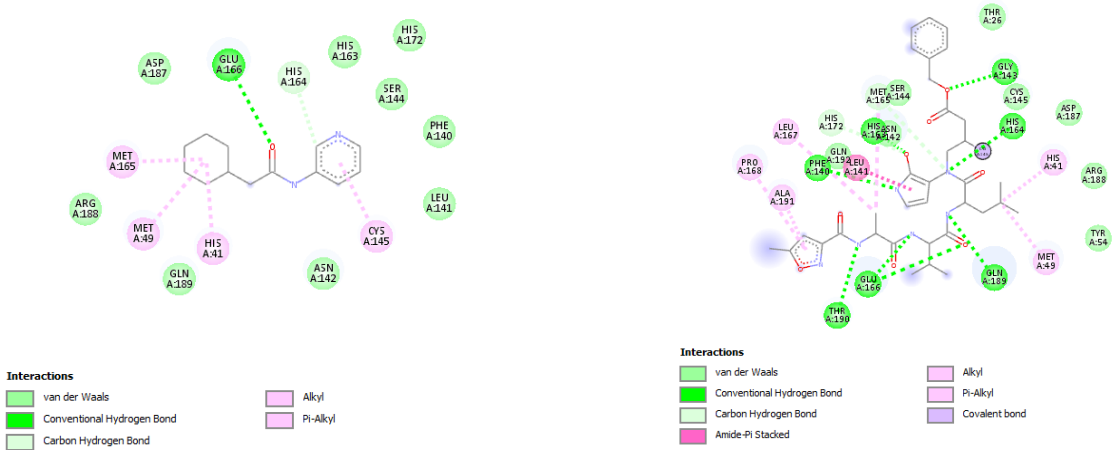

5R84 (Z31792168) 6LU7 (N3)

A: Native Ligand

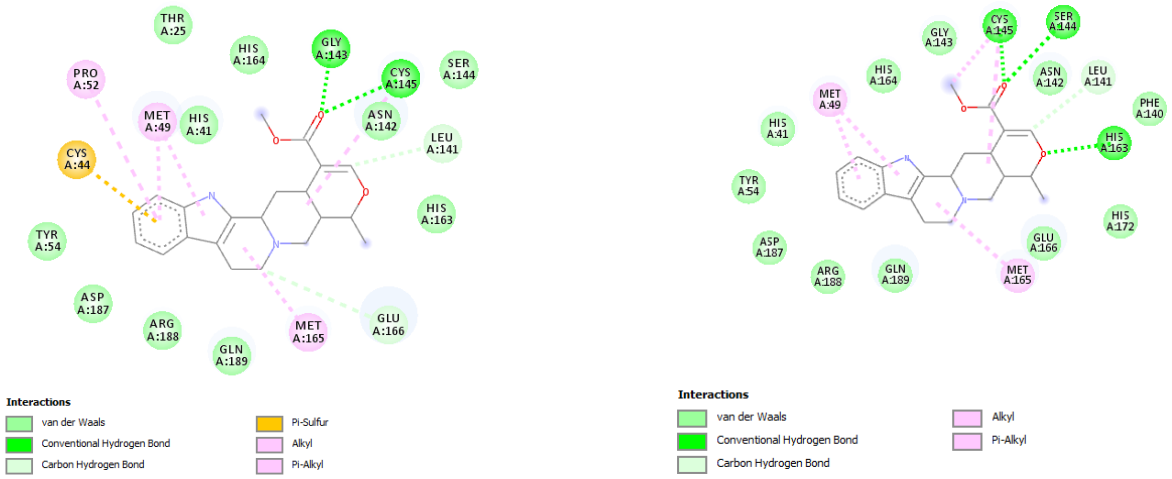

5R84 6LU7

B: Ajmalicine (28)

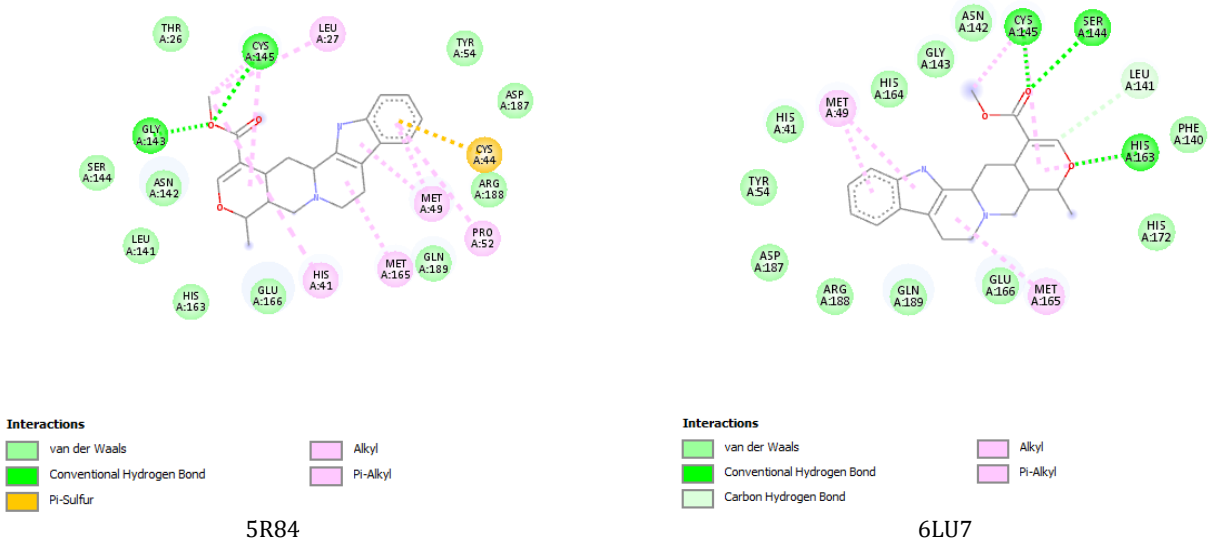

5R84 6LU7

C: Mitrajavine (29)

Figure 3. Ligand - Receptor interactions

Next, we assessed the interaction between ligands with the domain active site of the protein receptor, As can be seen in Figure 3, the binding mode of native ligand (Z31792168 and N3) on the active site domain of each macromolecule complex was observed based on its crystal structure. A native ligand of Z3179216855 in the active site of the protein receptor formed van der Walls interaction with HIS_{41} and alkyl interaction with CYS_{145}, also showed interaction with other residues including MET_{49}, PHE_{140}, LEU_{141}, ASN_{142}, SER_{144}, HIS_{163}, HIS_{164}, MET_{165}, GLU_{166}, HIS_{172}, ASP_{187}, ARG_{188}, and GLN_{189}. While, a native ligand of N3 in the active site of protein receptor formed Pi-alkyl interaction with HIS_{41} and covalent bond interaction with CYS_{145}, and has interaction with other residues including THR_{26}, MET_{49}, TYR_{54}, PHE_{140}, PHE_{141}, ASN_{142}, GLY_{143}, SER_{144}, HIS_{163}, MET_{165}, GLU_{166}, LEU_{167}, PRO_{168}, HIS_{172}, ASP_{187}, ARG_{188}, GLN_{189}, THR_{190}, ALA_{191} (Figure 3A).

As for ajmalicine (28), the binding site predicted on the active site of protein receptor 5R84 by Autodock 4.2.6 was formed based on van der Walls interaction with HIS_{41} and conventional hydrogen bond interaction with CYS_{145}. In addition to that, its interaction with some residues such as THR_{25}, CYS_{44}, MET_{49}, TYR_{54}, LEU_{141}, ASN_{142}, GLY_{143}, SER_{144}, HIS_{163}, HIS_{164}, MET_{165}, GLU_{166}, ASP_{187}, ARG_{188}, GLN_{189} were observed. Likewise, the binding site predicted on the active site of protein receptor 6LU7 by Autodock 4.2.6 was formed based on van der Walls interaction with HIS_{41}, three types (include alkyl, pi-alkyl, and conventional hydrogen bond) interaction with CYS_{145}, and also involved in the interaction with other residues including MET_{49}, TYR_{54}, PHE_{140}, LEU_{141}, ASN_{142}, GLY_{143}, SER_{144}, HIS_{163}, HIS_{164}, MET_{165}, GLU_{166}, HIS_{172}, ASP_{187}, ARG_{188}, GLN_{189} (Figure 3B).

Moreover, in the case of the protein receptors-mitrajavine (29) conformation, the binding site predicted on the active site of protein receptor 5R84 by Autodock 4.2.6 was formed based on pi-alkyl interaction with HIS_{41} and three types (alkyl, pi-alkyl, and conventional hydrogen bond) interaction with CYS_{145}, and other interaction with residues: THR_{26}, LEU_{27}, CYS_{44}, MET_{49}, PRO_{52}, TYR_{54}, LEU_{141}, GLY_{143}, SER_{144}, HIS_{163}, MET_{165}, GLU_{166}, ASP_{187}, ARG_{188}, GLN_{189}. Whereas, the binding site predicted on the active site of protein receptor 6LU7 by Autodock 4.2.6 was formed in a manner dependent on van der Walls interaction with HIS_{41}, three types (alkyl, pi-alkyl, and conventional hydrogen bond) interaction with CYS_{145}, and formed interaction with other residues including MET_{49}, TYR_{54}, PHE_{140}, LEU_{141}, ASN_{142}, GLY_{143}, SER_{144}, HIS_{163}, HIS_{164}, MET_{165}, GLU_{166}, HIS_{172}, ASP_{187}, ARG_{188}, GLN_{189} (Figure 3C). These *in silico* molecular docking studies have represented that HIS_{41} and CYS_{145} are the essential residues responsible for the main protease inhibition of the SARS-CoV-2 receptor. The molecular docking data indicated that mitrjavine and ajmalicine are a strong candidate of the main protease inhibitors of SARS-CoV-2.

Mitrajavine and ajmalicine included in monoterpenoid indole alkaloid group, and both compounds have almost the same structure, except they differ in the position of the hydrogen atoms bound to C_3, C_{15}, and C_{20} atoms [24]. Mitrajavine is a typical compound of the genus Mitragyna Korth, while ajmalicine can be found in some plants such as *M. spesiosa* leaves, roots of *V. rosea,* and *Rauwolfia spp* [33]. Scientific data from both compounds contained in *M. speciosa* leaves are still very limited, except for data from the mitragynine compound group [27,28,34,35]. Tran 1999 reported that the oral administration of ajmalicine extracted from the root of *V. rosea* (from 500 mg/kg to 1600 mg/kg) yielded no serious adverse effects, other than sedative, on mice. In addition to that, continuous oral administration in rabbits with high doses (4.8 mg/kg daily) did not affect the blood, body weight, and other biochemical indexes [36]. Meanwhile, a similar observation was obtained in the acute and subacute toxicity tests on *V. rosea* extract with various solvents [37,38,39]. Therefore, we believed that mitrajavine and ajmalicine will serve as suitable candidates for further research effort to examine their prospective anti-SARS-CoV-2 activities *in vitro* and *in vivo* prior to human trials for our future endeavor to combat COVID-19.

4 Conclusions

In the present study, we propose the potential use of mitrajavine and ajmalicine as the main protease of SARS-CoV-2 inhibitor,

based on the free energy binding and interaction conformation. Taken together, our results urge, the importance of new natural-derived compounds in drug discovery and their prospective antiviral activities against SARS-CoV-2. We further addressed the importance of *in silico* molecular docking study as one of important approaches in drug discovery to provide feasible predictions of biological activities and possible interactions of target compounds with host essential macromolecules (surface receptors, enzyme, ion channels, etc) in a rapid, accurate, and inexpensive manner.

5 Declarations

5.1 Acknowledgments

We are grateful to the Head of Pharmaceutical Research and Development Laboratory of "FARMAKA TROPIS" for providing facilities and financial supporting for our study.

5.2 Author Contributions

Islamudin Ahmad: writing manuscript; Nur Masyithah Zamruddin: Data Analysis; M. Arifuddin: Data and Literatur Collection; Yuspian Nur: Software prepare; and Firzan Nainu: English Proofreading.

5.3 Funding Statement

Pharmaceutical Research and Development Laboratory of "FARMAKA TROPIS".

5.4 Conflicts of Interest

All author declared that there is no conflict of interest

6 References

[1] Anonim. WHO Coronovirus Disease (COVID-19) Dashboard [Internet]. *World Health Organization*. 2020 [cited 2020 May 26]. Available from: https://covid19.who.int/?gclid=CjwKCAjw_LL2BRAkEiwAv2Y3SWqPVzvW6J2zszeR_R_fPXE-HDk_1xH1nq4XqQxFiFN09gO-CYgr6RoChhMQAvD_BwE

[2] Gallagher TM, Buchmeier MJ. Coronavirus Spike Proteins in Viral Entry and Pathogenesis. *Virology*, 2001; 374: 371–374.

[3] Chan JFW, To KKW, Tse H, Jin DY, Yuen KY. Interspecies transmission and emergence of novel viruses: Lessons from bats and birds. *Trends Microbiol*., 2013; 21(10): 544–555.

[4] Chan JF, Kok K, Zhu Z, Chu H, Kai-wang K, Yuan S, Yuen K. Genomic characterization of the 2019 novel human-pathogenic coronavirus isolated from a patient with atypical pneumonia after visiting Wuhan. *Emerg Microbes Infect*., 2020; 9: 221–236.

[5] Benvenuto D, Giovanetti M, Ciccozzi A, Spoto S, Angeletti S, Ciccozzi M. The 2019-new coronavirus epidemic: Evidence for virus evolution. *J Med Virol*., 2020; 92(4): 455–459.

[6] Rota PW, Oberste MS, Monroe SS, Nix WA, Campagnoli R, Icenogle JP, et al. Characterization of a novel coronavirus associated with severe acute respiraotry syndrome. *Science*. 2003; 300: 1953–1966.

[7] Gao J, Zhang L, Liu X, Li F, Ma R, Zhu Z, Zhang J, Wu J, Shi Y, Pan Y, Ge Y, Ruan K. Repurposing low-molecular-weight drugs against the main protease of SARS-CoV-2. *bioRxiv*. 2020; preprint

[8] Jan Bosch B, van der Zee R, de Haan CAM, Rottier PJM. The coronavirus spike protein is a class I virus fusion protein: Structural and functional characterization of the fusion core complex. *J Virol*., 2003; 77(16): 8801–8811.

[9] Md Fulbabu S, Rajarshi R, Nisha Amarnath J, Sayan P, Parimal K. Elucidating biophysical basis of binding of inhibitors to SARS-CoV-2 main protease by using molecular dynamics simulations and free energy calculations. *J Biomol Struct Dyn*., 2020; 1–30.

[10] Wang L, Wu Y, Deng Y, Kim B, Pierce L, Krilov G, Lupyan D, Robinson S, Dahlgren MK, Greenwood J, Romero DL, Masse C, Knight JL, Steinbrecher T, Beuming T, Damm W, Harder E, Sherman W, Brewer M, Wester R, Murcko M, Frye L, Farid R, Lin T, Mobley DL, Jorgensen WL, Berne BJ, Friesner RA, Abel R. Accurate and reliable prediction of relative ligand binding potency in prospective drug discovery by way of a modern free-energy calculation protocol and force field. *J Am Chem Soc.*, 2015; 137(7): 2695–2703.

[11] Jin Z, Du X, Xu Y, Deng Y, Liu M, Zhao Y, Zhang B, Li X, Zhang L, Peng C, Duan Y, Yu J, Wang L, Yang K, Liu F, Jiang R, Yang X, You T, Liu X, Yang X, Bai F, Liu H, Liu X, Gudat LW, Xu W, Xiao G, Qin C, Shi Z, Jiang H, Rao Z, Yang H. Structure of Mpro from COVID-19 virus and discovery of its inhibitors. *bioRxiv*., 2020; 2020.02.26.964882.

[12] Haider Z, Subhani MM, Farooq MA, Ishaq M, Khalid M, Khan RSA, Niazi AK. In silico discovery of novel inhibitors against main protease (Mpro) of SARS-CoV-2 using pharmacophore and molecular docking based virtual screening from ZINC database. *Preprints*. 2020; (March).

[13] Zhavoronkov A, Zhebrak A, Zagribelnyy B, Terentiev V, Bezrukov DS, Polykovskiy D, Shayakhmetov R, Filimonov A, Orekhov P, Yan Y., Popova O, Vanhaelen Q, Aliper A, Ivanenkov Y. Potential 2019-nCoV 3C-like protease inhibitors designed using generative deep learning approaches potential COVID-19 3C-like protease inhibitors designed using generative deep learning approaches. *chemrxiv.*, 2020; 307(2): E1.

[14] Mirza MU, Froeyen M. Structural elucidation of SARS-CoV-2 vital proteins: Computational methods reveal potential drug candidates against main protease, Nsp12 polymerase and Nsp13 helicase. *J Pharm Anal*. 2020 ; *in press*.

[15] Liu S, Zheng Q, Wang Z. Potential covalent drugs targeting the main protease of the SARS-CoV-2 coronavirus. *Bioinformatics*. 2020; btaa224: 1–4.

[16] Colson P, Rolain JM, Raoult D. Chloroquine for the 2019 novel coronavirus SARS-CoV-2. *Int J Antimicrob Agents*., 2020; 55(3): 105923.

[17] Senathilake KS, Samarakoon SR, Tennekoon KH. Virtual screening of inhibitors against spike glycoprotein of SARS-CoV2: a drug repurposing approach. *Preprints*, 2020; (March).

[18] Wang Q, Zhao Y, Chen X, Hong A. Virtual screening of approved clinic drugs with main protease (3CLpro) reveals potential inhibitory effects on SARS-CoV-2. *Preprints*. 2020; (March).

[19] Chen H, Du Q. Potential natural compounds for preventing SARS-CoV-2 (2019-nCoV) infection. *Preprints*. 2020; 2(March).

[20] Serseg T, Benarous K, Yousfi M. Hispidin and Lepidine E : Two natural compounds and folic acid as potential inhibitors of 2019-novel coronavirus main protease (2019- nCoVM pro), molecular docking and SAR study. *arXiv*, 2020; 2004.08920.

[21] Utomo RY, Ikawati M, Meiyanto E. Revealing the potency of citrus and galangal constituents to halt SARS-CoV-2 infection. *Preprints*. 2020;2(March):1–8.

[22] Rao P, Shukla A, Parmar P, Goswami D. Proposing a fungal metabolite-Flaviolin as a potential inhibitor of 3CLpro of novel coronavirus SARS-CoV2 using docking and molecular dynamics. *arXiv*. 2020; 2004.03806.

[23] Zhang MZ, Chen Q, Yang GF. A review on recent developments of indole-containing antiviral agents. *Eur J Med Chem*. 2015; 89: 421–441.

[24] Brown PN, Lund JA, Murch SJ. A botanical, phytochemical and ethnomedicinal review of the genus Mitragyna korth: Implications for products sold as kratom. *J Ethnopharmacol*. 2017; 202: 302–325.

[25] Shaik Mossadeq WM, Sulaiman MR, Tengku Mohamad TA, Chiong HS, Zakaria ZA, Jabit ML, Baharuldin MTH, Israf DA. Anti-inflammatory and antinociceptive effects of *Mitragyna speciosa* Korth methanolic extract. *Med Princ Pract*. 2009; 18(5): 378–384.

[26] Sabetghadam A, Ramanathan S, Sasidharan S, Mansor SM. Subchronic exposure to mitragynine, the principal alkaloid of *Mitragyna speciosa*, in rats. *J Ethnopharmacol*. 2013; 146(3): 815–823.

[27] Mohd Moklas MA, Suliman NA, Mat Taib CN, Baharuldin MTH. Sedative, cognitive impairment and anxiolytic effects of acute *Mitragyna speciosa* in rodents. *J US-China Med Sci*. 2013; 10(1): 37–44.

[28] Parthasarathy S, Azizi JB, Ramanathan S, Ismail S, Sasidharan S, Mohd MI, et al. Evaluation of antioxidant and antibacterial activities of aqueous, methanolic and alkaloid extracts from *Mitragyna speciosa* (rubiaceae family) leaves. *Molecules*, 2009; 14(10): 3964–3974.

[29] Boyle NMO, Banck M, James CA, Morley C, Vandermeersch T, Hutchison GR. Open Babel : An open chemical toolbox. *J Cheminform*., 2011; 3(33): 1–14.

[30] Morris GM, Huey R, Lindstrom W, Sanner MF, Belew RK, Goodsell DS, Oslon AJ. AutoDock4 and AutodockTools4: Automated docking with selectivity receptor flexibility. *J Comput Chem*. 2009; 30(16): 2785–2791.

[31] BIOVA DS. Discovery Studio Visualizer. San Diego, USA; 2020.

[32] Wu C, Liu Y, Yang Y, Zhang P, Zhong W, Wang Y, Wang Q, Xu Y, Li M, Li X, Zheng M, Chen L, Li H. Analysis of therapeutic targets for SARS-CoV-2 and discovery of potential drugs by computational methods. *Acta Pharm Sin B*., 2020; 10(5): 766-788

[33] Anonim. Ajmalicine [Internet]. National Library of Medicine. 2020 [cited 2020 May 30]. Available from: https://pubchem.ncbi.nlm.nih.gov/compound/Ajmalicine

[34] Ramanathan S, Parthasarathy S, Murugaiyah V, Magosso E, Tan SC, Mansor SM. Understanding the physicochemical properties of mitragynine, a principal alkaloid of *Mitragyna speciosa*, for preclinical evaluation. *Molecules*, 2015; 20(3): 4915–4927.

[35] Kumarnsit E, Keawpradub N, Nuankaew W. Acute and long-term effects of alkaloid extract of *Mitragyna speciosa* on food and water intake and body weight in rats. *Fitoterapia*, 2006; 77(5): 339–345.

[36] Tran T Van. Study on acute and subacute toxicity of ajmalicin extracted from root of

Catharanthus roseus G. Don. *Pharm J*. 1999; 282(10): 14–17.

[37] Das MC, Reddy M, Prabodh S, Sunethri P. Evaluation of acute oral toxicity of ethanol leaves extract of *Catharanthus roseus* in wistar albino rats. *J Clin Diagnostic Res*., 2017; 11(3): 12–15.

[38] Kevin LYW, Hussin AH, Zhari I, Chin JH. Sub-acute oral toxicity study of methanol leaves extract of *Catharanthus roseus* in rats. *J Acute Dis*., 2012; 2012: 38–41.

[39] Roy S, Chatterjee P. A non-toxic antifungal compound from the leaves of Catharanthus roseus characterized as 5-hydroxy flavone by UV spectroscopic analysis and evaluation of its antifungal property by agar-cup method. *Ind Crop Prod*., 2010; 32(3): 375–380.